

"This is the peer reviewed version of the following article:

"A Stable Quasi-Solid-State Sodium-Sulfur Battery"

which has been published in final form at

<https://onlinelibrary.wiley.com/doi/abs/10.1002/anie.201805008>

This article may be used for non-commercial purposes in accordance with [Wiley Terms and Conditions for Self-Archiving](#)

A Stable Quasi-Solid-State Sodium–Sulfur Battery

Dong Zhou, Yi Chen, Baohua Li,* Hongbo Fan, Faliang Cheng, Devaraj Shanmukaraj, Teofilo Rojo, Michel Armand,* and Guoxiu Wang*

Abstract: Ambient-temperature sodium–sulfur (Na–S) batteries are considered a promising energy storage system due to their high theoretical energy density and low costs. However, great challenges remain in achieving a high rechargeable capacity and long cycle life. Herein we report a stable quasi-solid-state Na–S battery enabled by a poly(*S*-pentaerythritol tetraacrylate (PETEA))-based cathode and a (PETEA-tris[2-(acryloyloxy)ethyl] isocyanurate (THEICTA))-based gel polymer electrolyte. The polymeric sulfur electrode strongly anchors sulfur through chemical binding and inhibits the shuttle effect. Meanwhile, the *in situ* formed polymer electrolyte with high ionic conductivity and enhanced safety successfully stabilizes the Na anode/electrolyte interface, and simultaneously immobilizes soluble Na polysulfides. The as-developed quasi-solid-state Na–S cells exhibit a high reversible capacity of 877 mA h g⁻¹ at 0.1 C and an extended cycling stability.

Sodium batteries are considered to be suitable for large-scale energy storage due to the natural abundance of Na.^[1] Among Na battery systems, sodium–sulfur (Na–S) batteries based on a conversion chemistry have drawn tremendous attention because of the high energy density and low cost of sulfur (S) cathodes.^[2] Traditional Na–S batteries, firstly commercialized in 2002, operate at high temperature (300–350 °C) with molten electrodes and sodium β-alumina solid electrolyte. Such high-temperature Na–S batteries can deliver a theoretical energy density of 760 Wh kg⁻¹ as well as a long cycling life. However, Na polysulfides (Na₂S_{*n*}, *n* ≥ 3) in a liquid state are the final discharge products of this battery

system, which causes a low utilization (only ca. 1/3) of the theoretical capacity of sulfur.^[3] Additionally, the high operating temperature not only imposes additional costs for operation and maintenance, but also creates serious safety risks, which significantly impedes the applications of high-temperature Na–S batteries.^[3] In contrast, ambient-temperature Na–S batteries have unique advantages such as increased theoretical energy density (1274 Wh kg⁻¹ considering Na₂S as the final discharge product) and enhanced safety.^[4] However, ambient-temperature Na–S batteries still face many intrinsic obstacles. These include the poor electrical conductivity of sulfur and its huge volumetric variation (ca. 170%) during cycling, the shuttle of highly soluble Na polysulfides, the poor kinetics of conversion from short-chain Na polysulfides or Na₂S to long-chain polysulfides, and the uncontrollable growth of Na dendrites. All these result in low reversible capacity, serious self-discharging and poor cycle stability.^[5]

To enhance the electrochemical performance of ambient-temperature Na–S batteries, intensive efforts have been devoted to confine sulfur into carbon matrix with the aim of improving electronic conductivity and restraining the shuttle of polysulfides.^[6] However, the physical confinement of polysulfides in such S@C hybrids alone is insufficient for overcoming the shuttle effect. Therefore, the rational design of a cathode structure that introduces a strong chemical binding in the S@C hybrids is crucially important for developing high-performance Na–S batteries. Meanwhile, replacing traditional liquid electrolyte (LE) with solid polymer electrolyte has attracted particular attention since it can simultaneously slow the diffusion of dissolved polysulfides, and eliminate safety issues (such as fire and explosion) caused by the leakage of flammable solvents.^[7] Unfortunately, the Na–S batteries with polymer electrolytes generally suffer from large polarization and rapid capacity decay, owing to the low ionic conductivity of polymer electrolytes and the unstable electrode/polymer electrolyte interfaces.

Herein, we employ star-shaped crosslinking monomers to prepare polymeric sulfur cathode and gel polymer electrolyte (GPE), and successfully fabricate stable quasi-solid-state Na–S batteries. The strong chemical binding between sulfur and polymer framework in the S-rich copolymer electrode effectively confines Na polysulfides inside the cathode. The functional GPE formed via *in situ* synthesis not only possesses high ionic conductivity, a stable Na anode/GPE interface without dendrite formation and enhanced safety, but also provides strong chemical interaction between the functional groups on copolymer matrix and Na polysulfides to efficiently suppress the shuttle effect. Thus, the as-developed quasi-solid-state Na–S cells deliver a high specific capacity of 877 mA h g⁻¹ at 0.1 C with a stable cyclability.

[*] Dr. D. Zhou, Y. Chen, Prof. G. Wang
Centre for Clean Energy Technology
School of Mathematical and Physical Sciences
University of Technology Sydney
Sydney, NSW 2007 (Australia)
E-mail: Guoxiu.Wang@uts.edu.au

Prof. B. Li
Graduate School at Shenzhen, Tsinghua University
Shenzhen, Guangdong 518055 (China)
E-mail: libh@mail.sz.tsinghua.edu.cn

Prof. H. Fan, Prof. F. Cheng
School of Materials Science and Engineering
Dongguan University of Technology
Dongguan, Guangdong 523106 (China)

Dr. D. Shanmukaraj, Prof. T. Rojo, Prof. M. Armand
CIC ENERGIGUNE, Parque Tecnológico de Álava
Miñano 01510 (Spain)
E-mail: amarmand@cicenergigune.com

Supporting information and the ORCID identification number(s) for the author(s) of this article can be found under:
<https://doi.org/10.1002/anie.201805008>.

Figure 1 shows the fabrication procedure of the quasi-solid-state Na-S batteries. Firstly, poly(S-pentaerythritol tetraacrylate (PETEA)) copolymer was prepared via inverse vulcanization-like process. In this process, molten sulfur was

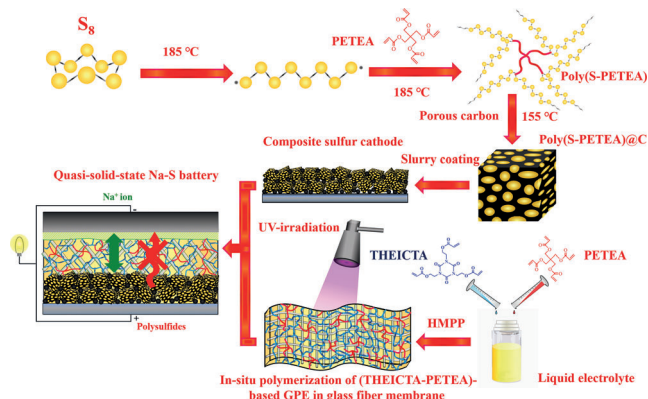


Figure 1. Schematic illustration of the preparation of the quasi-solid-state Na-S battery.

heated to 185 °C to convert the eight-membered ring sulfur molecule into linear structure with the ends of diradical chains, and then copolymerized with PETEA to form the S-rich poly(S-PETEA) (see Figure S1 in the Supporting Information). Subsequently, the as-prepared poly(S-PETEA) was infiltrated into a MOF-5-derived mesoporous carbon host (Figure S2) to obtain the poly(S-PETEA)@C that improves the electrical conductivity of polymeric sulfur. To prepare the GPE, PETEA and tris[2-(acryloyloxy)ethyl] isocyanurate (THEICTA) monomers together with 2-hydroxy-2-methyl-1-phenyl-1-propanone (HMPP) photo-initiator were dissolved in a 1 M sodium bis(trifluoromethane)sulfonimide (NaTFSI) in propylene carbonate (PC): fluoroethylene carbonate (FEC) (1:1 by volume) to form a precursor solution, and then subjected to a ultraviolet light (UV)-irradiation to initiate the radical polymerization of C=C bonds of the monomers in a glass fiber membrane (Figure S3). Finally, a cross-linked (PETEA-THEICTA)-based GPE was in situ constructed (Figure S4). The poly(S-PETEA)@C cathode, (PETEA-THEICTA)-based GPE and Na metal were integrated together to fabricate quasi-solid-state Na-S cells. It is noted that the symmetrical star structures of PETEA and THEICTA possess more than three active sites (i.e., C=C bonds) in each molecule, which enable the preparation of copolymer cathode and GPE with very small amounts of added monomers (< 3 wt %).

As shown in Figure S5a, the as-prepared poly(S-PETEA) copolymer presents a sulfur content of 97.1 wt % determined by thermogravimetric analysis (TGA). NMR and X-ray photoelectron spectroscopy (XPS) measurements were conducted to confirm the formation of such copolymer via detecting the presence of C–S bonds. The ^1H NMR spectrum of poly(S-PETEA) in Figure 2a exhibits resonances at 2.5–2.8 ppm and 3.4–3.7 ppm, corresponding to the methylene and methyne peaks in the PETEA matrix bonded to sulfur comonomer units.^[8] As shown from the XPS results in Figure 2b, the S 2p peaks of sulfur are well-fitted by three peaks

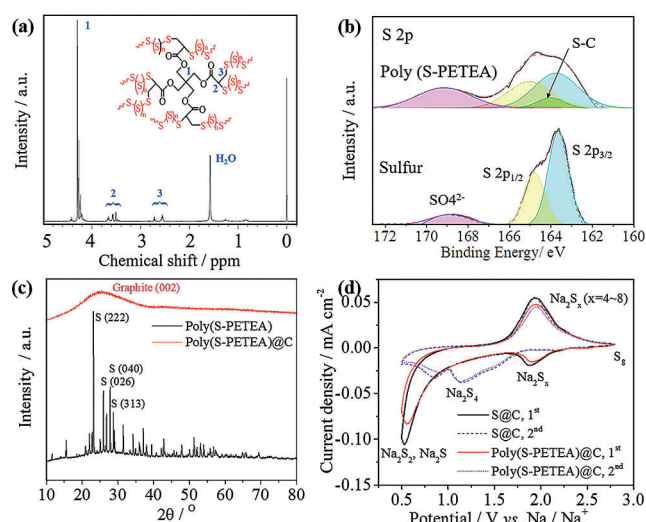


Figure 2. Characterization of the poly(S-PETEA)-based cathode. a) ^1H -NMR spectrum of poly(S-PETEA); b) S 2p XPS spectra of sulfur and poly(S-PETEA); c) XRD patterns of poly(S-PETEA) and poly(S-PETEA)@C; d) CV curves of Na/LE/S@C and Na/LE/poly(S-PETEA)@C cells at 0.1 mVs $^{-1}$.

at around 163.6, 164.8 eV and 168.8 eV, which can be assigned to S 2p $_{3/2}$, S 2p $_{1/2}$, and sulphate species, respectively.^[9] A new peak appearing at around 163.8 eV in the spectrum of poly(S-PETEA) is related to a S–C bond generated by the successful copolymerization.^[10] This is further validated by the C 1s spectrum of poly(S-PETEA) (Figure S6b). Therefore, the formation of poly(S-PETEA) copolymer with strong covalent C–S bonds was successfully achieved.

The poly(S-PETEA) was further composited with mesoporous carbon host to obtain poly(S-PETEA)@C hybrid. X-ray diffraction (XRD) was performed to investigate the crystal phase changes from poly(S-PETEA) to poly(S-PETEA)@C hybrid. The XRD pattern of the poly(S-PETEA) in Figure 2c indicates the existence of long-chain elemental sulfur with an orthorhombic structure (S-PDF#08-0247) in the copolymer. In contrast, the peak intensity of sulfur can hardly be observed in the poly(S-PETEA)@C hybrid, which signifies a complete physical confinement of polymeric sulfur inside the mesoporous carbon.^[11] Cyclic voltammetry (CV) was performed to compare the electrochemical characteristics of S@C and poly(S-PETEA)@C electrodes in ambient-temperature Na-S cells employing 1 M NaTFSI in PC:FEC as electrolyte. As shown in Figure 2d, the poly(S-PETEA)@C electrode shows very similar CV curves to that of the S@C electrode. This verifies that the poly(S-PETEA) copolymer exhibits similar electrochemical characteristic to bare S $_8$. A current slope starts at around 2.1 V versus Na/Na $^+$ during the initial cathodic scan of the poly(S-PETEA)@C cell, which is related to the reduction of $[-\text{S}_n-]$ chains in the polymeric sulfur and its subsequent solid–liquid transition to form dissolved Na $_2\text{S}_x$ ($x = 4-8$).^[2] The peak at 1.2–0.5 V corresponds to the generation of Na $_2\text{S}$ and Na $_2\text{S}_2$ within the PETEA-based polymer matrix, which shows limited repeatability in the following cathodic sweep, indicating an incomplete conversion of such solid products. This is

mainly because of the kinetically difficult conversions from solid-state short-chain polysulfides or Na_2S to long-chain polysulfides.^[12] During the anodic scan, only a repeatable peak at around 2.1 V assigned to the reversible transformation from short-chain sodium sulfides to long-chain polysulfides appears over all cycles.^[3] It is expected that the embedding of polymer matrix in the poly(S-PETEA) not only acts as an intrinsic binder, but also chemically confines Na polysulfides during cycling (Figure S7).^[13]

Figure 3 a shows the Fourier transform infrared spectroscopy (FTIR) spectra of the PETEA monomer, THEICTA monomer and the polymer matrix of (PETEA-THEICTA)-based GPE obtained by removing LE from the GPE. Peaks at 1168 cm^{-1} (C–O, symmetrical stretching), 1724 cm^{-1} (C=O stretching) and 1684 cm^{-1} (isocyanurate ring stretching) appear in the spectra of monomers. It is seen that the peak

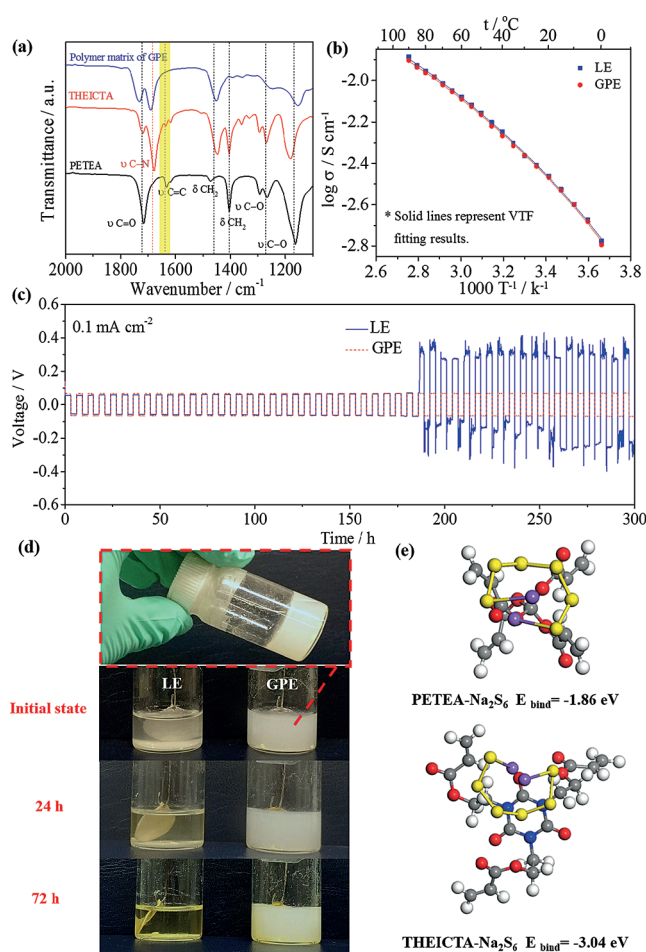


Figure 3. Characterization of the (PETEA-THEICTA)-based GPE. a) FTIR spectra of PETEA and THEICTA monomers, and the polymer matrix of GPE; b) The ionic conductivities of LE and GPE as a function of temperature. The plots represent the experimental data meanwhile the solid lines represent VTF fitting results. c) Galvanostatic cycling curves of Na/Na symmetrical cells using LE or GPE at a current density 0.1 mA cm^{-2} . d) Visual observation of Na polysulfides formation and diffusion in LE and GPE with different aging time. e) Calculated binding energies of Na_2S_6 with PETEA and THEICTA monomers. Yellow, purple, gray, white, red and blue balls represent sulfur, sodium, carbon, hydrogen, oxygen and nitrogen atoms, respectively.

at approximately 1637 cm^{-1} assigned to the stretching vibration of C=C bonds nearly disappears in the spectrum of GPE matrix.^[14] This indicates that the monomers have been polymerized in LE with a high degree of conversion.

Ionic conductivity is a core parameter for polymer electrolytes applied in energy storage devices.^[15] We measured the ionic conductivities for the (PETEA-THEICTA)-based GPE film and the blank LE (1M NaTFSI in PC:FEC) as a function of temperature from 0 to 90°C . The GPE possesses a high conductivity of $3.85 \times 10^{-3}\text{ S cm}^{-1}$ at 25°C (Figure 3 b and Table S1), which is almost the same as that of the LE ($3.90 \times 10^{-3}\text{ S cm}^{-1}$). Such high ionic conductivity value is sufficient to meet the requirement for solid-state Na-S batteries. As shown in Figure S8, the Na ion transference number (T_{Na^+}) of (PETEA-THEICTA)-based GPE reaches 0.34, which is obviously higher than that of the LE (0.27). This may be due to a fact that the copolymerized PETEA-THEICTA framework greatly limits the movement of anions.^[15] Such improved T_{Na^+} of GPE is expected to not only reduce the polarization of polymer batteries,^[16] but also increase the Sand's time and result in a stable electrodeposition of Na.^[17] This is validated by galvanostatic cycling measurements performed on a symmetric Na/Na cell at a current density of 0.1 mA cm^{-2} . As shown in Figure 3 c, for the Na/LE/Na cell, the voltage hysteresis between the voltages of Na stripping and plating obviously rises after about 170 h, indicating a deteriorated Na/LE interface caused by the accumulated thick solid electrolyte interface (SEI) layer and Na dendrite growth.^[18] In contrast, the Na/GPE/Na cell exhibits a much lower voltage fluctuation and remains stable up to 300 h, which demonstrates a uniform Na deposition with a stable Na/GPE interface without the safety hazards caused by dendrite growth. The GPE also has much enhanced electrochemical and thermal stabilities compared to LE (Figures S9–10).

To directly characterize the formation and diffusion of Na polysulfides in electrolytes, visual observation on the same amount of sulfur powder together with a Na foil soaked in LE or GPE was performed. The LE turns a yellow color after aging at 60°C for 72 h (Figure 3 d). Such distinct color change implies that the sulfur powder continuously dissolves in the LE and then electrochemically reacts with Na metal to generate soluble Na polysulfides with dark colors, corresponding to the self-discharge phenomenon in cells.^[19] However, the GPE remains milky white during the aging process, indicating that the dissolution of polysulfides has been dramatically alleviated in the GPE. First-principle calculations were further employed to analyze the interaction between Na polysulfides and the copolymer matrix of GPE. The binding energy between Na_2S_6 as a representative of Na polysulfides and ester group-rich PETEA monomer is calculated to be -1.86 eV (Figure 3 e). More impressively, the THEICTA monomer with a isocyanurate ring on its structure exhibits a binding energy with Na_2S_6 as high as -3.04 eV . Such binding energy values are much stronger than that of PC- Na_2S_6 (-1.57 eV) and FEC- Na_2S_6 (-1.22 eV). As a result, Na_2S_6 molecules are preferentially immobilized by the functional groups in the copolymer matrix of GPE rather than diffuse in the electrolyte solvents, which leads to a low

solubility of Na polysulfides in the GPE. Therefore, the outcome of theoretical calculation is coincident with the above experimental result. The CV of Na/GPE/poly(S-PETEA)@C cell shown in Figure S11 indicates the highly reversible reactions in the GPE.

Figure 4a,b shows the rate performances of the Na/GPE/poly(S-PETEA)@C cell from 0.1 to 2 C and corresponding discharge/charge curves. It is seen from Figure 4a that the discharge/charge potential gaps of the Na/GPE/poly(S-PETEA)@C cell at various rates are obviously smaller than those of the Na/LE/S@C (Figure S12a) and Na/LE/poly(S-PETEA)@C (Figure S12b) cells. This suggests that the combination of poly(S-PETEA)-based electrode and (PETEA-THEICTA)-based GPE can remarkably decrease the polarization of ambient-temperature Na-S batteries. Furthermore, the Na/GPE/poly(S-PETEA)@C cell delivers specific charge capacities of 877, 762, 629, 495 and 372 mAhg⁻¹ at 0.1, 0.2, 0.5, 1 and 2 C, respectively, which are obviously higher than the Na/LE/S@C and Na/LE/poly(S-PETEA)@C cells. The capacity retention of the Na/GPE/poly(S-PETEA)@C cell is calculated as 91.4% of the starting value when the current density was switched back to 0.1 C. So, this novel quasi-solid-state Na-S battery is highly robust and stable (Figure 4b). Cycling tests were also measured at a current density of 0.1 C shown in Figure 4c. For the Na/

GPE/poly(S-PETEA)@C cell, high Coulombic efficiency (ca. 100%) and limited capacity decay are obtained. The reversible capacity is 736 mAhg⁻¹ after 100 cycles, and the corresponding energy density (calculated based on the mass of sulfur) is around 956 Whkg⁻¹ based on a mid-value discharge voltage of about 1.3 V. In sharp contrast, the reversible capacities for the Na/LE/S@C and Na/LE/poly(S-PETEA)@C cells after 100 cycles are only 373 and 517 mAhg⁻¹, respectively. This can be attributed to an inhibition of polysulfide shuttle and a stability of the electrode/GPE interface in the Na/GPE/poly(S-PETEA)@C cell (Figures S13,14).

The Na anodes disassembled from Na-S cells after 100 cycles are characterized by field emission scanning electron microscopy (FE-SEM). Massive dendrite structures and holes can be clearly observed on the surface of the Na anode obtained from the Na/LE/S@C cell (Figure 4d); meanwhile the sulfur content on such anode is as high as 8.96 wt%. The Na anode from the Na/LE/poly(S-PETEA)@C cell shows a sulfur content of 3.36 wt% (Figure S15). With the combination of polymeric sulfur cathode and functional GPE, as expected, the surfaces of Na anodes tend to be smooth and the growth of Na dendrite is markedly suppressed. The sulfur content on the anode of Na/GPE/poly(S-PETEA)@C cell is as low as 0.96 wt% (Figure 4e), validating a successful inhibition of shuttle effect.

As shown in Figure 4f, the electrochemical performance of the Na/GPE/poly(S-PETEA)@C battery in this work is obviously better than previously reported ambient-temperature Na-S batteries using polymer electrolytes or polymeric sulfur electrodes. The high energy density, good cycling stability and enhanced safety of this quasi-solid-state Na-S battery make it a promising low-cost energy storage system.

In conclusion, we have successfully applied star-shaped crosslinking monomers to design polymeric sulfur electrode and functional polymer electrolyte for fabricating quasi-solid-state Na-S batteries. The poly(S-PETEA)-based electrode effectively confines sulfur via chemical binding and suppress the polysulfide shuttle. The (PETEA-THEICTA)-based GPE with high ionic conductivity and improved safety not only strongly immobilizes Na polysulfides against diffusion into the electrolyte solvents, but also benefits for the formation of a stable Na/GPE interface upon cycling. Such dual optimization of cathode and electrolyte enables a stable cycling of quasi-solid-state Na-S cells with high energy density. This work offers a new pathway for the development of low-cost and high-performance ambient-temperature Na-S batteries.

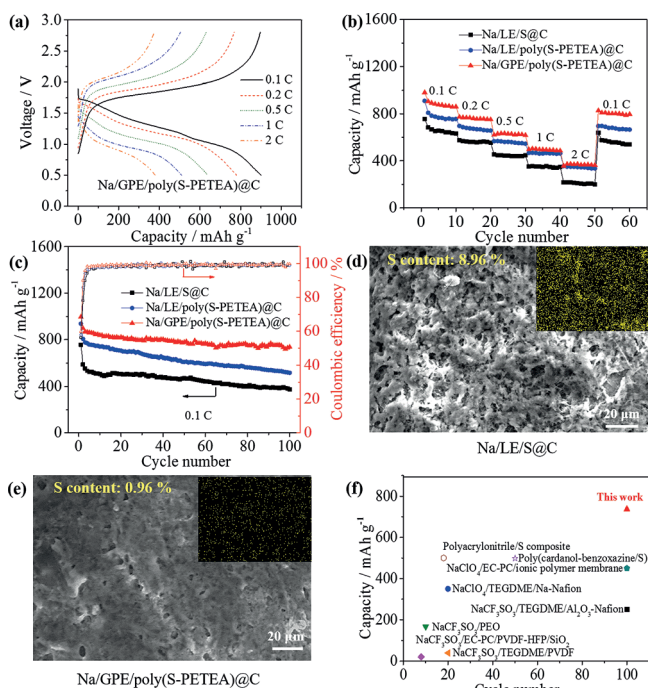


Figure 4. Electrochemical performance of the quasi-solid-state Na-S batteries. a) Typical charge/discharge profiles of Na/GPE/poly(S-PETEA)@C cells. b) Rate performances and c) cycling performances at 0.1 C of Na/LE/S@C, Na/LE/poly(S-PETEA)@C and Na/GPE/poly(S-PETEA)@C cells; The FE-SEM images and corresponding elemental maps of sulfur (shown in insets) of Na anodes obtained from d) Na/LE/S@C and e) Na/GPE/poly(S-PETEA)@C cells after 100 cycles at 0.1 C. f) Comparison of the practical specific capacities and cycling performances for representative reported ambient-temperature Na-S batteries employing polymer electrolytes (solid symbols)^[7a,b,20] or polymeric sulfur electrodes (hollow symbols)^[21] and this work.

Acknowledgements

We would like to acknowledge the support by the Australian Renewable Energy Agency project (ARENA 2014/RND106) and the ARC Discovery Project (DP170100436). We thank Dr. Peng Li from Nanjing University of Aeronautics and Astronautics for conducting the first-principle calculations.

Conflict of interest

The authors declare no conflict of interest.

Keywords: gel polymer electrolytes · polymeric sulfur electrodes · shuttle effects · sodium dendrites · sodium–sulfur batteries

-
- [1] X. Chen, X. Shen, B. Li, H. J. Peng, X. B. Cheng, B. Q. Li, X. Q. Zhang, J. Q. Huang, Q. Zhang, *Angew. Chem. Int. Ed.* **2018**, *57*, 734–737; *Angew. Chem.* **2018**, *130*, 742–745.
- [2] Y.-X. Wang, J. Yang, W. Lai, S.-L. Chou, Q.-F. Gu, H. K. Liu, D. Zhao, S. X. Dou, *J. Am. Chem. Soc.* **2016**, *138*, 16576–16579.
- [3] S. Wei, S. Xu, A. Agrawal, S. Choudhury, Y. Lu, Z. Tu, L. Ma, L. A. Archer, *Nat. Commun.* **2016**, *7*, 11722.
- [4] K. B. Hueso, M. Armand, T. Rojo, *Energy Environ. Sci.* **2013**, *6*, 734–749.
- [5] Y.-X. Wang, B. Zhang, W. Lai, Y. Xu, S.-L. Chou, H.-K. Liu, S.-X. Dou, *Adv. Energy Mater.* **2017**, *7*, 1602829.
- [6] a) S. Xin, Y. X. Yin, Y. G. Guo, L. J. Wan, *Adv. Mater.* **2014**, *26*, 1261–1265; b) R. Carter, L. Oakes, A. Douglas, N. Muralidharan, A. P. Cohn, C. L. Pint, *Nano Lett.* **2017**, *17*, 1863–1869; c) Z. Qiang, Y.-M. Chen, Y. Xia, W. Liang, Y. Zhu, B. D. Vogt, *Nano Energy* **2017**, *32*, 59–66.
- [7] a) C.-W. Park, H.-S. Ryu, K.-W. Kim, J.-H. Ahn, J.-Y. Lee, H.-J. Ahn, *J. Power Sources* **2007**, *165*, 450–454; b) C.-W. Park, J.-H. Ahn, H.-S. Ryu, K.-W. Kim, H.-J. Ahn, *Electrochem. Solid-State Lett.* **2006**, *9*, A123–A125; c) X. Li, K. Qian, Y.-B. He, C. Liu, D. An, Y. Li, D. Zhou, Z. Lin, B. Li, Q.-H. Yang, *J. Mater. Chem. A* **2017**, *5*, 18888–18895; d) D. Xu, D. Chao, H. Wang, Y. Gong, R. Wang, B. He, X. Hu, H. J. Fan, *Adv. Energy Mater.* **2018**, *8*, 1702769; e) J.-Z. Guo, A.-B. Yang, Z.-Y. Gu, X.-L. Wu, W.-L. Pang, Q.-L. Ning, W.-H. Li, J.-P. Zhang, Z.-M. Su, *ACS Appl. Mater. Interfaces* **2018**, *10*, 17903–17910.
- [8] W. J. Chung, J. J. Griebel, E. T. Kim, H. Yoon, A. G. Simmonds, H. J. Ji, P. T. Dirlam, R. S. Glass, J. J. Wie, N. A. Nguyen, *Nat. Chem.* **2013**, *5*, 518.
- [9] a) M. Liu, D. Zhou, Y.-B. He, Y. Fu, X. Qin, C. Miao, H. Du, B. Li, Q.-H. Yang, Z. Lin, *Nano Energy* **2016**, *22*, 278–289; b) C. Y. Fan, Y. P. Zheng, X. H. Zhang, Y. H. Shi, S. Y. Liu, H. C. Wang, X. L. Wu, H. Z. Sun, J. P. Zhang, *Adv. Energy Mater.* **2018**, *8*, 1703638.
- [10] K. Shen, H. Mei, B. Li, J. Ding, S. Yang, *Adv. Energy Mater.* **2018**, *8*, 1701527.
- [11] G. Hu, Z. Sun, C. Shi, R. Fang, J. Chen, P. Hou, C. Liu, H. M. Cheng, F. Li, *Adv. Mater.* **2017**, *29*, 1603835.
- [12] X. Yu, A. Manthiram, *J. Phys. Chem. C* **2014**, *118*, 22952–22959.
- [13] F. Wu, S. Chen, V. Srot, Y. Huang, S. K. Sinha, P. A. Aken, J. Maier, Y. Yu, *Adv. Mater.* **2018**, *30*, 1706643.
- [14] a) P. Petrov, M. Bozukov, C. B. Tsvetanov, *J. Mater. Chem.* **2005**, *15*, 1481–1486; b) B. Perret, B. Schartel, K. Stöb, M. Ciesielski, J. Diederichs, M. Döring, J. Krämer, V. Altstädt, *Eur. Polym. J.* **2011**, *47*, 1081–1089.
- [15] E. Quartarone, P. Mustarelli, *Chem. Soc. Rev.* **2011**, *40*, 2525–2540.
- [16] D. Zhou, R. Liu, J. Zhang, X. Qi, Y.-B. He, B. Li, Q.-H. Yang, Y.-S. Hu, F. Kang, *Nano Energy* **2017**, *33*, 45–54.
- [17] P. Bai, J. Li, F. R. Brushett, M. Z. Bazant, *Energy Environ. Sci.* **2016**, *9*, 3221–3229.
- [18] D. Zhou, R. Liu, Y. B. He, F. Li, M. Liu, B. Li, Q. H. Yang, Q. Cai, F. Kang, *Adv. Energy Mater.* **2016**, *6*, 1502214.
- [19] D. Zhou, M. Liu, Q. Yun, X. Wang, Y. B. He, B. Li, Q. H. Yang, Q. Cai, F. Kang, *Small* **2017**, *13*, 1502214.
- [20] a) D. Kumar, M. Suleman, S. Hashmi, *Solid State Ionics* **2011**, *202*, 45–53; b) I. Bauer, M. Kohl, H. Althues, S. Kaskel, *Chem. Commun.* **2014**, *50*, 3208–3210; c) E. Ceylan Cengiz, Z. Erdol, B. Sakar, A. Aslan, A. Ata, O. Ozturk, R. D. Cakan, *J. Phys. Chem. C* **2017**, *121*, 15120–15126; d) S. Wei, S. Choudhury, J. Xu, P. Nath, Z. Tu, L. A. Archer, *Adv. Mater.* **2017**, *29*, 1605512.
- [21] a) A. Ghosh, S. Shukla, M. Monisha, A. Kumar, B. Lochab, S. Mitra, *ACS Energy Lett.* **2017**, *2*, 2478–2485; b) T. H. Hwang, D. S. Jung, J.-S. Kim, B. G. Kim, J. W. Choi, *Nano Lett.* **2013**, *13*, 4532–4538.

Manuscript received: May 3, 2018

Accepted manuscript online: June 26, 2018

Version of record online: ■ ■ ■ ■, ■ ■ ■ ■ ■ ■ ■ ■

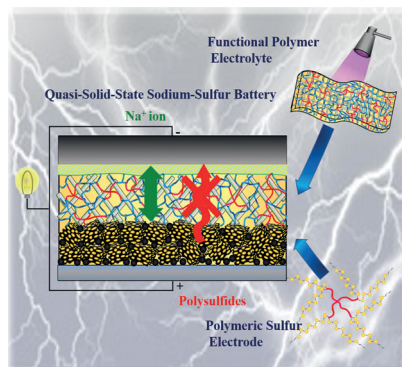
Communications



Nanoelectrochemistry

D. Zhou, Y. Chen, B. Li,* H. Fan, F. Cheng,
D. Shanmukaraj, T. Rojo, M. Armand,*
G. Wang* ————— ■■■■-■■■■

A Stable Quasi-Solid-State Sodium–
Sulfur Battery



Energy storage: A stable quasi-solid-state Na–S battery has been obtained using a poly(S-pentaerythritol tetraacrylate (PETEA)) cathode and a (PETEA-tris[2-(acryloyloxy)ethyl] isocyanurate (THEICTA)) gel polymer electrolyte. The electrode strongly anchors sulfur by chemical binding, meanwhile the polymer electrolyte with high ionic conductivity and stable Na/electrolyte interface effectively suppresses the shuttle of polysulfides.